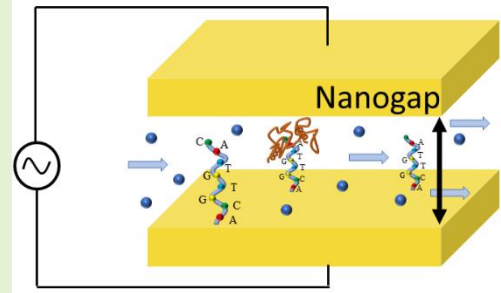


A Tutorial on Electrochemical Impedance Spectroscopy and Nanogap Electrodes for Biosensing Applications

N.T. Kemp

Abstract—Electrochemical Impedance Spectroscopy (EIS) is a powerful measurement technique used by scientists and engineers to characterize and understand the interfacial behavior of liquid-solid interfaces. Such investigations are important in numerous applications and fields of research, including electrochemical synthesis and deposition of materials, such as metals and conducting polymers, corrosion protection analysis, investigation of molecule-surface interactions, and research on batteries and fuel cells. In recent years, advances in nanotechnology have led to a rise in the use of EIS in chemical and bio-sensing. Areas such as molecular diagnostics and healthcare can greatly benefit from this novel technology, which includes low-cost, rapid response measurements that can be done by non-experts at the point of care. For new entrants, the depth of knowledge and breadth of EIS and its many applications can be rather daunting. This article therefore serves as a tutorial on basic EIS theory, whilst highlighting new applications in advanced bio-sensing. The tutorial begins with a theoretical overview, including electrical AC impedance, formation and structure of electrical double layers at liquid solid-interfaces and equivalent circuit models used to represent interfacial phenomena. This is followed by an introduction to bio-sensing and a review of recent research highlights on resistive and capacitive biosensors based on nanogap electrodes, especially those having novel applications from DNA detection to nanoparticle capturing. Lastly, the article highlights a recent new breakthrough on how the combination of nanogap electrodes with label-free methods, such as aptamer functionalized surfaces, can make capacitive sensors with extremely high sensitivity and specificity.

Index Terms — Electrochemical Impedance Spectroscopy (EIS), electrode double layer (EDL), capacitive biosensor, nanogap electrodes, AC impedance, aptamer, label-free



I. Introduction

THE development of nanotechnology over the last few decades have led to an extraordinary rate of new advances in chemical and bio-sensing. Detection capabilities have reached levels as high as attomole (10^{-18}) sensitivity [1][2][3][4] with very high specificity and sensor types have gone from requiring large labs and expensive analytical equipment and methods to small, portable hand-held sensors that are low cost and simple to operate [5][6]. Many new advances are still developing in the field, as new materials are created and our understanding of the electrical, optical, magnetic and mechanical properties of new nanostructures is extended with continued discoveries.

Electrochemical Impedance Spectroscopy (EIS) is a powerful measurement technique that is increasingly being exploited in new chemical and bio-sensing technologies. However, the fundamentals and practices of EIS is often not taught in the subject disciplines of users, which is nowadays broad and covers physicists, chemists, biologists and engineers. This article therefore serves as both, a tutorial for new entrants

to the field, and an overview of new developments in biosensing, especially nanogap electrodes for detecting analytes with extremely high sensitivity and specificity.

This article begins by reviewing electrical impedance in AC circuits and the concept of a “phase shift” between the potential across a circuit element and the current passing through it. After a description of basic AC theory, the topic of impedance effects in ionic solutions is introduced. In contrast to solid-state systems, whose ions remain stationary under normally electric field strengths, ionic solutions differ in that their ions are mobile. Their migration towards the electrodes in the solution leads to so-called electrode polarization effects and the creation of an electrical double layer (EDL) that drastically changes the dielectric properties of the liquid-solid interface. This has considerable implications for EIS in biosensing applications.

Following on from the tutorial section, the article explores new nanotechnology-based advances in biosensing. In particular, the use of nanoscale architectures for enhancing device sensitivity. The main type considered are those utilizing nanogap electrodes, which consist of a pair of electrodes separated by a very small nanometer-scale gap. When

combined with surface functionalization, sensors can be made, that not only have very high sensitivity but are label-free and highly specific to the biomolecule to be detected.

II. BASIC AC CIRCUIT THEORY

Readers already familiar with this topic may wish to skip directly to § III Electrochemical Impedance Spectroscopy.

In contrast to direct current DC circuits in which the applied potential (voltage) is static in nature, alternating current AC circuits have a potential that varies in time in a periodic manner. The waveform is typically sinusoidal, but it can also be triangular, square wave, sawtooth, pulsed, or have a more complex form. The behavior of AC circuits is very different to DC circuits. In DC circuits, except for transient conditions (such as those that occur when turning a circuit on or off), the behavior of circuit elements such as resistors, capacitors and inductors are generally constant and are described as being in the steady-state. Since the current is constant, inductors can be considered as normal conducting wires and capacitors can be considered as open circuits. However, in the case of unbiased AC circuits (those having no DC offset so that their mean potential is zero) the applied potential difference is continuously switching between positive and negative potential, so the current in the circuit is constantly changing direction. As capacitors and inductors are essentially energy storage devices, the changing potential difference causes them to repeatedly switch between storing energy and releasing it. The main effect of this is that the current through inductors and capacitors is out of phase with the potential difference across them, as shown in Fig. 1.

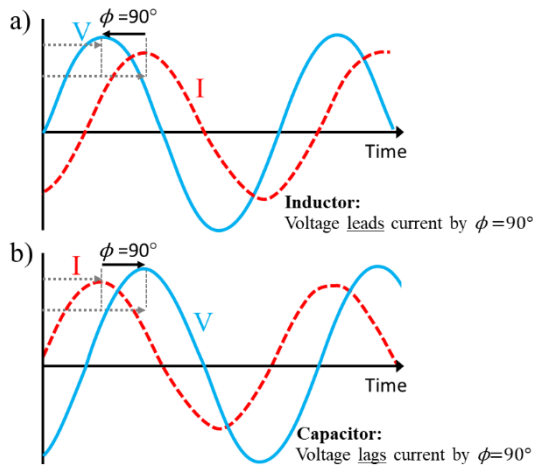


Fig. 1. The phase relationship between the potential different (voltage) across a circuit element and current through it. a) shows the case for an inductor where voltage is said to lead the current by 90° and b) shows the case for a capacitor where voltage lags the current by 90° .

The phase is different depending on the component type. For example, since an inductor acts to resist the change in the current (by creating a back electromotive force that opposes the voltage), the current in an inductor builds more slowly than the voltage across it, when a potential is first applied. Therefore, the voltage leads the current in time and phase with $\phi = 90^\circ$. In contrast, since a capacitor is a charge storage device and the

current must first add charge onto the capacitor for it to function, the current is said to be driving the behavior of the capacitor. In this case, the potential difference across a capacitor (voltage) is said to lag the current in both time and phase with $\phi = 90^\circ$. Because of these effects, the overall electrical “resistance” of AC circuits containing inductors and capacitors can be no longer considered constant but has a nature that is dynamic. To distinguish this electrical “resistance” from the static resistance in a DC circuit, the terminology of “impedance” is then used.

In understanding AC circuits, it is helpful to use phasor diagrams as a means to visualize the phase difference between the voltage and current in capacitors and inductors. Phasors can be treated in the same manner as vectors and can be added together to determine the overall impedance of a circuit that contains a number of inductors, capacitors and resistors. These types of circuits are abbreviated as RLC, RL or RC circuits and they can have either a series or parallel configuration. In a phasor diagram, the usual reference point for zero phase is the horizontal axis and in the case of an RLC series circuit, this is associated with the phase of the current of the resistor in the circuit, since in a series RLC circuit the current is common to all three components. [Note: In the case of an RLC parallel circuit, it is the voltage that is common to all three circuit components and the vector diagram instead uses voltage as its reference and has the current vectors of the components plotted with respect to the voltage]. Phasor diagrams for a series RLC circuit are shown in Fig. 2 and consist of phasors for the current (I) and voltage across the resistor (V_R), inductor (V_L) and capacitor (V_C). The various phases are represented by angles drawn relative to the horizontal reference vector. The angular frequency (ω) is related to the frequency of the supply by $\omega = 2\pi f$, and the sense of direction is taken as being anti-clockwise for the rotation of the phasors.

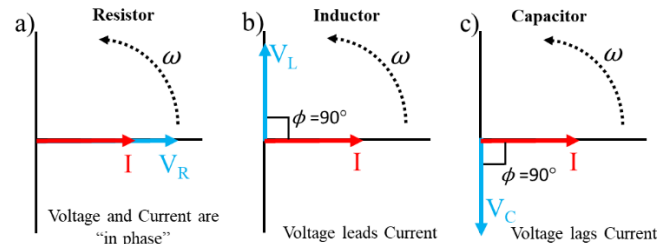


Fig. 2. Phasor diagrams for the a) resistor, b) inductor and c) capacitor when in a series RLC circuit.

In Fig. 3, the circuit schematic and vector phasor addition of a simple series RLC circuit is presented. The impedance of the circuit can be determined by applying Kirchoff’s voltage law to the circuit, as shown in equation (1). Since it is a series circuit, the sum of the individual circuit elements and the voltage source, (V_S), must equate to zero.

$$V_S - V_R - V_L - V_C = 0 \quad (1)$$

From the phasor diagram, Fig. 3b, V_S can be determined by combining the three phasors V_R , V_L , V_C using vector addition and Pythagoras’s theorem in equation (2)

$$V_S = \sqrt{V_R^2 + (V_L - V_C)^2} \quad (2)$$

$$V_S = \sqrt{(IR)^2 + (IX_L - IX_C)^2}$$

$$V_S = I\sqrt{R^2 + (X_L - X_C)^2}$$

where X_L and X_C are the individual reactance's of the inductor and capacitor respectively.

Finally, in analogy with Ohm's law for a DC circuit, where $V = IR$, it can be seen in equation (3) and Fig. 3c that the voltage of the source is proportional to the current through the circuit multiplied by a proportionality constant, which is the total impedance of the circuit.

$$V_S = IZ \quad (3)$$

$$\text{where } Z = \sqrt{R^2 + (X_L - X_C)^2}$$

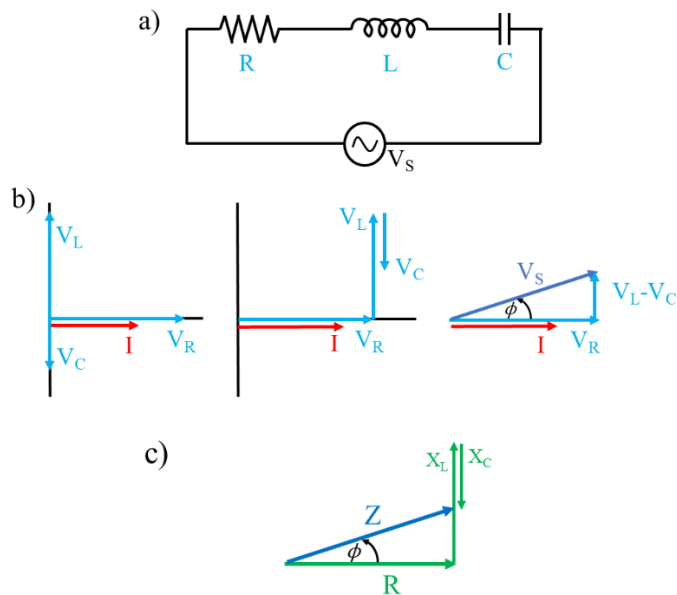


Fig. 3. a) Schematic of a series RLC circuit and b) vector phasor addition of the individual components to give the source voltage and c) total circuit impedance.

The phase angle, ϕ , between the source voltage and current of the series circuit, I , can be determined as follows:

$$\tan\phi = \frac{X_L - X_C}{R} \quad (4)$$

It can also be seen that the RLC circuit has a resonance when the impedance of the circuit is a minimum, which occurs when $X_L = X_C$. In this case the impedance of the circuit is purely real, i.e. $Z = R$.

Furthermore, since $X_L = \omega L$ and $X_C = \frac{1}{\omega C}$, the resonance condition can be seen in (5) as follows:

$$\begin{aligned} X_L &= X_C \\ \omega L &= \frac{1}{\omega C} \\ \omega &= \sqrt{\frac{1}{LC}} \end{aligned} \quad (5)$$

III. ELECTROCHEMICAL IMPEDANCE SPECTROSCOPY

Electrochemical Impedance Spectroscopy (EIS) is a non-destructive, steady-state measurement method that enables the monitoring of dielectric relaxation phenomena over a wide frequency spectrum, typically in the range 10^{-4} to 10^6 Hz. The method is typically quick and simple to perform and has the advantage of both, real-time and *in situ* measurement [5]. The origins of EIS are embedded within the study of interfacial electrical phenomenon at an electrode-liquid surface and go all the way back to Volta [7] in 1800, who showed that an electrode-electrolyte interface was the source of an electrical potential and that this could be used as a battery to provide DC electricity. During these times it was suspected that the electrode-electrolyte interface had the property of capacitance and this was first demonstrated in 1871 by Varley [8], who performed a series of experiments with platinum plates dipped in a mixture of sulphuric acid and water. He was particularly impressed by the sheer size of the measured capacitance.

A. Circuit Model Descriptions

Circuit model descriptions based on the properties of known circuit elements played an enormous role in helping to understand the electrode-electrolyte interface. The first steps towards developing a circuit model approach and understanding the electrode-solution interface capacitance through an equivalent electrical circuit model came in 1879, when Helmholtz [9] proposed that a double layer of charge existed at an electrode-electrolyte interface, as shown in Fig. 4a. He proposed the double layer consisted of positive and negative charges separated by a short distance that resembled the capacitive nature of measurements on these systems.

It was to be another 20 years until this simple model was improved upon when Emil Warburg [10] in 1899, determined that upon application of a very small current, the magnitude of the capacitance (C_W) varied inversely with the square root of frequency (f) and that the reactance was equal to the resistance ($X_W = R_W$) with the phase angle constant at 45 degrees, as shown in Fig. 4b. He introduced the concept that at low current density the interface is better represented by a series circuit consisting of a capacitor and resistor. However, this simple series model falsely predicted an infinite impedance in the case of a direct current (zero frequency) measurement and therefore lacked a mechanism for charge transfer across the capacitor, known as a Faradaic resistance.

Further improvement upon this early model did not come until much later. In 1932, Fricke [11] reported that the polarization capacitance and phase angle were actually dependent on the metal and electrolyte species and varied as $C_P \sim \omega^{-m}$ and $\phi = m\pi/2$, respectively, and with m typically varying between 0.15 and 0.32, as shown in Fig. 4c. Then in 1947, experimental work by John Randles [12] led to the development of an equivalent electrical circuit consisting of a double-layer Helmholtz capacitance (C_P) in parallel with a "Faradaic" impedance, consisting of a resistance (R) and capacitance (C), as shown in Fig. 4d.

The Randles cell became particular well-known because of

its simplicity and inclusion of all of the main elements of an electrochemical interface. Nowadays, the Randles cell is more commonly depicted as that shown in Fig. 4e. It consists of the double layer capacitance (C_{dl}) in parallel with a series combination of the charge transfer resistance (R_{ct}) and Warburg (W) element. The Warburg element is used to specifically represent the electrochemical reaction at redox active sites and relates to the delay arising from the diffusion of the electroactive species to the electrode surface. This representation of the Randles Cell also includes the resistance of the electrolyte (R_s). Because of its simplicity, the Randles cell is still very popular to this day. It is often used as a starting point for determining the different parameters in an unknown electrochemical system, or used as a basis for developing a more complex model. However, real electrochemical systems are typically more complicated and other equivalent circuit models may need to be sought for the specific application involved.

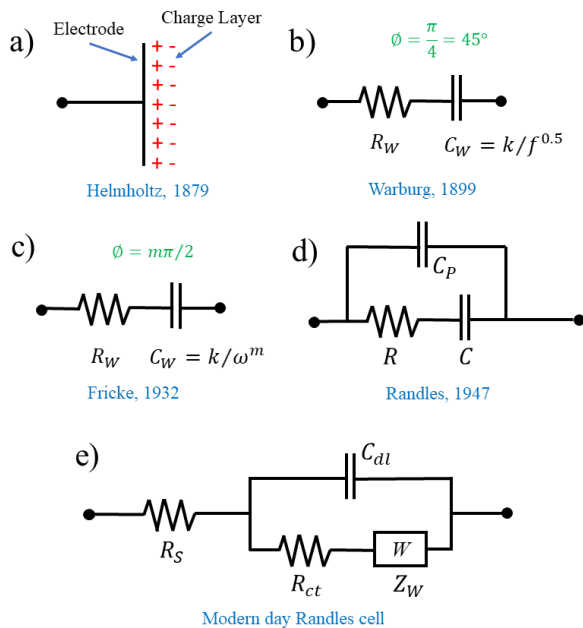


Fig. 4. a) Helmholtz double layer and the b) Warburg circuit model with additional improvements by c) Fricke and d) Randles. e) Modern day Randles cell, which includes the resistance of the electrolyte (R_s) in series with a parallel combination of the double layer capacitance (C_{dl}), charge transfer resistance (R_{ct}) and Warburg element (Z_W). The Warburg element represents the process of electrochemical diffusion.

B. The Nature of the Electrical Double Layer

The nature of the electrical double layer itself has been the subject of intense research and refinement from its early description first proposed by Helmholtz [9][13] in 1853-79, where it was described as being of a compact layer of polarized dipoles located very close to the surface of the electrodes. Later in 1913, Gouy-Chapman [14][15] developed a more diffuse layer approach by taking into consideration the thermal motion of the ions. According to this model the potential drop across the diffuse layer decreases exponentially as a function of distance with a characteristic length given by the Debye length (λ_D) (or Debye-Hückel parameter) as follows:

$$\lambda_D = \sqrt{\frac{\epsilon_r \epsilon_0 k_B T}{2N_A e^2 I}} \quad (6)$$

where ϵ_r is the dielectric constant (or relative permittivity), ϵ_0 is the permittivity of free space, k_B is the Boltzmann constant, T is the temperature, N_A is the Avogadro number, e is the elementary charge and I is the ionic strength of the electrolyte (in mol m^{-3}).

In 1924, Stern [16] took the approach of combining the main elements of both the Helmholtz and the Gouy-Chapman models to give an improved description of the EDL. This model, sometimes known as the Gouy-Chapman-Stern (GCS), consists of both a compact Helmholtz layer and the diffuse layer of Gouy-Chapman. Further refinement and models for more specific electrolytes and electrode materials followed in subsequent years. A significant contribution was the work of Grahame [17] in 1957, who for aqueous solutions found it necessary to include a contribution to the properties of the double layer arising from the surface change of water dipoles. To this day, this Grahame model in combination with the Gouy-Chapman equation provides an overall accurate description of the EDL for most aqueous electrolytes. It is valid for most metal types and also many non-aqueous solvents.

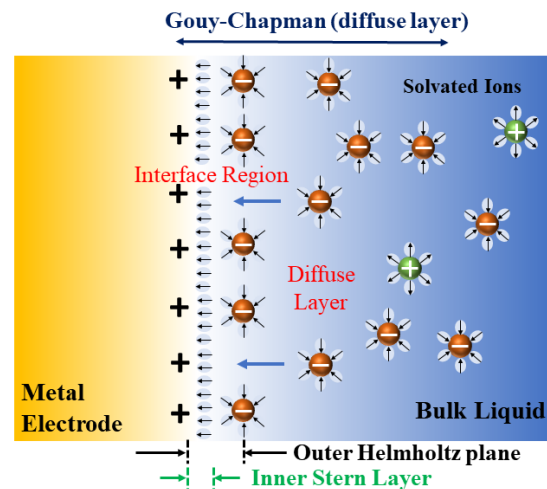


Fig. 5. Structure of the Electrical Double Layer made from the contributions of Helmholtz, Stern, Gouy and Chapman.

C. Practical Techniques

Nowadays, EIS is used to study a wide range of interfacial phenomena such as corrosion kinetics, surface reactions and studies on the electrochemical deposition and synthesis of a wide range of materials. Typically, a potentiostat is used to apply a small signal sinusoidal voltage with fixed amplitude across a 3-electrode cell containing an electrolyte. The three electrodes are called the Working, Reference and Counter Electrode. In some setups, additional connections may be used which include a Working Sense and / or Counter Sense, or in some applications, the measurement process is simplified by using a 2-electrode set up in which the counter electrode is tied to the reference electrode.

The Working Electrode is typically the main electrode of interest for either the study of its own surface properties, or for understanding electrochemical reactions that take place in its

vicinity. The electrode must be conducting and either be made from the material of interest itself or be coated with the material to be studied. The working electrode is the electrode where the reduction or oxidation reactions occurs and these are initiated by applying a DC offset to the AC measurement probe (e.g. a DC potential + small AC sine wave).

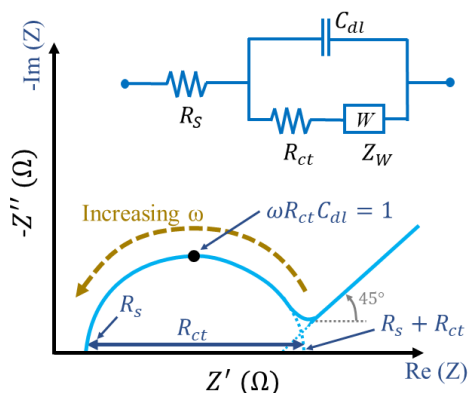


Fig. 6. By plotting the imaginary impedance ($-Z''$) vs. the real impedance (Z'), the Nyquist Plot enables determination of the charge transfer (R_{ct}) and solution resistance (R_s) of the Randles Cell. The presence of a Warburg impedance can be seen by the straight line with a 45° angle to the abscissa.

The Counter Electrode supplies the current and the Reference Electrode defines a well-known and stable potential reference. There are many types of reference electrodes. The more commonly used types are the Standard hydrogen electrode (SHE), Silver chloride electrode (AgCl) and Saturated calomel electrode (SCE) and these have specific advantages for different types of measurement applications.

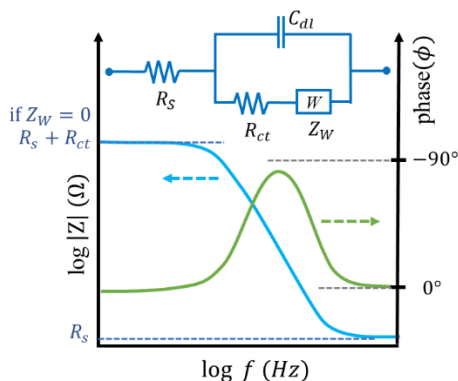


Fig. 7. A Bode Plot combines a plot of log impedance and phase vs. log frequency. The example shown is for a simplified Randles Cell that has no Warburg diffusion element. In this case a simple characteristic shape is observed for the impedance and phase. At low frequency the impedance is the series sum of the solution resistance and the charge transfer resistance. At high frequency the total impedance becomes just the solution resistance.

Obtaining an EIS spectra typically involves applying a small sinusoidal potential whilst measuring the current and sweeping slowly across a range of frequencies, typically from a few Hz (or mHz) to hundreds of kHz (or a few MHz). The resulting data can be plotted in a variety of ways. The most common approaches are Nyquist plots, typified by plotting the imaginary impedance (Z'') vs. the real impedance (Z'), and Bode plots, which involve plotting the magnitude of the impedance ($|Z|$) and/or phase angle, (ϕ) vs. the frequency (ω) on a log-log plot.

The Nyquist plot, although more complex, has the advantage that the charge transfer resistance, Warburg impedance and time constants can be easily determined, as shown in Fig. 6. A Bode plot, Fig. 7, has the advantage that the main measurement data is presented on a single plot and the plot better highlights the effect of frequency on the capacitance and phase.

There are two main EIS approaches that are used in biosensing applications, Faradaic and non-Faradaic. In a non-Faradaic method there is ideally no electron transfer between the electrodes and the main focus is on detecting changes in the capacitance double layer, which because of its close location near to the electrode surface can be used to detect binding of bio-markers to electrodes functionalized with bio-recognition elements such as aptamers, anti-bodies or enzymes (see Fig.9 for different types of surface capture probes).

In contrast, Faradaic approaches use electrolytes containing a high concentration of reduction-oxidation (redox) species that undergo reversible electrochemical reactions (driven by the applied voltage) and increase electron transfer across the liquid-electrode interface. A commonly used redox probe is ferri/ferro-cyanide $[\text{Fe}(\text{CN})_6]^{3-/4-}$, which undergoes the reaction:

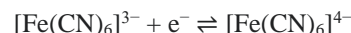


Fig. 8. shows a typical example of how Faradaic electron transfer can be utilized in bio-sensing applications. In this example, the electrode surface is functionalized with a label-free capture probe that will only bind to the specific target molecule. The black and grey curves on the Nyquist plot are EIS spectra of the sensor before and after exposure to the solution containing the target biomolecule, respectively. With increasing uptake of the non-conductive target molecules by the capture probes, redox reactions between the electrolyte and the electrode surface are increasingly blocked. The reduction in the electron transfer reactions causes the charge transfer resistance (R_{ct}) of the electrochemical cell to increase, which can be seen in the Nyquist plot as an increase in the radius of the semicircle portion of the curve.

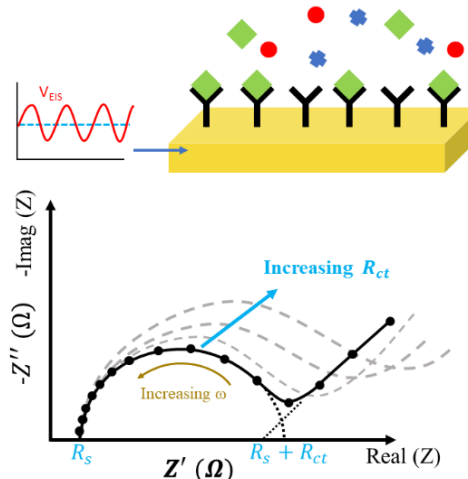


Fig. 8. A Nyquist plot of an EIS Faradaic process. Increased binding events of the specific target molecule with the capture probe-functionalized electrode blocks redox reactions between the electrolyte and the electrode surface. The reduction in electron transfer causes the charge transfer resistance (R_{ct}) of the electrochemical cell to increase. The increase in R_{ct} can be seen in the Nyquist plot as an increase in the radius of the semicircle portion of the curve.

Other types of experiments that are also relevant in electrochemistry are cyclic voltammograms (CV). A CV is a potentiodynamic measurement that involves measuring the current whilst applying a DC potential that is ramped linearly from a negative potential to a positive potential and back again in a cyclical manner. The rate of voltage change over time is known as the scan rate (V/s). The potential is measured between the working electrode and the reference electrode, whilst the current is measured between the working electrode and the counter electrode. The data is plotted as current (I) vs applied potential (E or V). Peaks and troughs in the CV can be used to identify redox reactions (reduction and oxidation), as shown in Fig. 9. During the scan, redox chemical reactions generate an additional Faradaic current whilst the accumulation of ions on the electrodes (charging) leads to a much smaller capacitive current that usually has a rectangular profile of very thin width (see red dotted line in Fig. 9). If subtraction of the capacitive current is desired, a CV scan with just the electrolyte solution and containing no Faradaic species can be performed and subtracted after the main experiment. Typically, however, the capacitive current is small and can often be ignored.

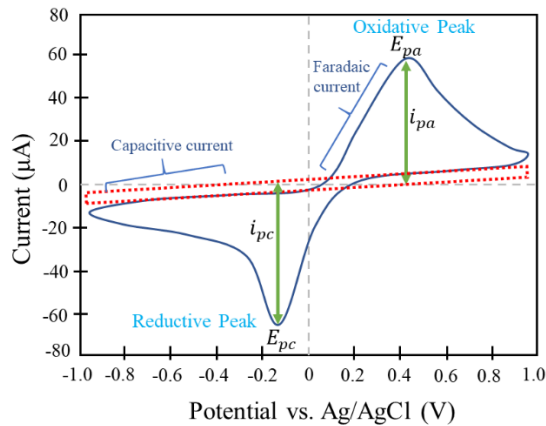


Fig. 9. A cyclic voltammogram showing the presence of an electrochemical redox reaction that is characterized by reduction (cathodic) and oxidation (anodic) peaks at E_{pc} and E_{pa} respectively and associated cathodic (i_{pc}) and anodic current (i_{pa}).

IV. EIS IN BIOSENSING APPLICATIONS

Many traditional methods for the detection of analytes are lab-based and involve large and expensive equipment, such as mass spectrometers or polymerase chain reaction (PCR) analysis stations. In the last decade, enormous research efforts have been made to develop new sensor technologies that are portable, easy to use and low cost. Because of new advances in nanotechnology involving the design, fabrication and understanding of new phenomena at the nanoscale, electronic impedance-based sensing has gained enormous attention because it offers the ability to make electronic chip-sized sensors that are ultra-small, highly-sensitive and can be manufactured in their thousands at low cost. Such systems are highly desirable in applications, where in-field measurement and fast speed of analysis are essential. Applications are numerous such as water quality testing, monitoring of

foodstuffs and industrial bioprocesses, detection of biological agents used in warfare and numerous applications in medicine.

Medical applications represent an enormous area of opportunity, especially relevant nowadays because of the increasing strain on most medical systems due to aging populations. Low-cost, portable sensor analysis systems can have a high degree of impact in point-of-care applications and telemonitoring, where they can significantly decrease waiting times and remove bottlenecks within the system, and free up the valuable and expensive time of professional clinical staff for other tasks. Point-of-care or with-patient testing enables medical staff to achieve lab-quality diagnostics within minutes rather than hours or days and allows for quick decision making and better monitoring of a patient's condition, as well as response to medicine and treatment. In remote or telemonitoring, the patient can be at home or carrying out their life as normal, whilst being monitored in real-time, and their test results transmitted wirelessly to their electronic medical record for review by their clinician.

Much of the recent progress in EIS biosensing has been brought about by advances in nanoscale engineering in conjunction with surface functionalization methods for immobilization and detection [18]. These have driven many of the improvements in biosensor design, function and operation. Electrochemical [19] and field effect transistor [20] approaches are central to many of the technologies developed, but new types are still emerging such as memristor-based Si nanowire sensors, which have achieved extraordinary levels of sensitivity with detection levels as low as 23 attomole [3].

A. EIS Label-free methods

One particular advantage of impedance based biosensing is the direct detection of the target analyte using label-free methods. Currently, most biosensor types require a label to be attached to the target species to be detected. The label, often a fluorophore, nanoparticle, magnetic bead, biotin or enzyme enables a method of detecting the presence of the target through the detection of the label, which is usually easier to detect. For example, in the case of a fluorophore, the fluorophore label (or fluorescent tag) attaches to the target species if it is present in the sample. After a washing procedure, simple illumination by UV light can then be used to reveal the presence of the target, which is indicated by fluorescent glow of the molecular tag. However, labelling is generally a disadvantage because it requires additional materials and steps to be undertaken in the preparation and testing procedure. This increases the time and cost of the process. Labelling can also drastically change the properties of a biomolecule. For example, it can change how a protein functions and how it binds to other species, which may mean the protein cannot be used for other processes or tests. Furthermore, whilst labelling is relatively straightforward and reliable in the case of DNA, the uptake of a label for proteins is more complicated and highly dependent on their shape, size and molecular structure.

In label-free impedance biosensors the target species is directly detected by its presence within the device, usually through changes in the electrical resistance or dielectric constant. Since uptake of the target species can be rapid, label-

free approaches also offer real-time monitoring. The label-free method generally involves the use of functionalized surfaces that interact within the target species, typically immobilizing it close to the surface where the electrical resistance path or dielectric volume is modified. No labels are needed since the surface is functionalized with compounds that directly interact with the target species. Materials typically used for functionalization of the surface in biosensing include antibodies, aptamers, enzymes and streptavidin, as shown in Fig. 10. These usually need to be modified in some way so that they can be anchored by a surface. A common modification is the attachment of a thiol group, which binds strongly to gold. Other covalent binding approaches support attachment to silicates and silicon substrates and involve first the functionalization of the surface with hydroxyl, amine or carboxylic acid followed by chemical reaction processes to attach desired probes [21].

Whilst label-free methods have many advantages, they are not without problems. Label-free methods tend to be more prone to errors introduced by the run conditions (e.g. temperature, user) than labelled methods and this is compounded by the signaling, which is often small and requires significant amplification. Label-free methods also suffer from a significant degree of non-specific adsorption (especially at high analyte concentrations). This obscures target binding to the capture probe, which leads to an increase in the background signal and a decrease in the overall sensitivity.

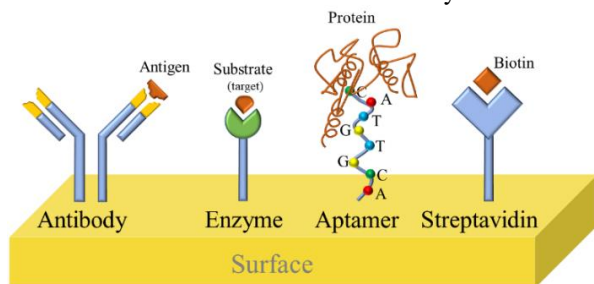


Fig. 10. Different methods of surface functionalization for the label-free detection of target analytes.

B. Aptamers

Each of the capture probes given in Fig. 10 have various advantages for their intended application. For brevity, we only discuss Aptamers in this review. Aptamers are short, single-stranded DNA or RNA molecules that have a high affinity to organic molecules and proteins. Their main advantages for use in bio-sensing is their stability in harsh experimental environments, very high specificity to a particular target analyte and reversible binding properties. Their specificity comes from their chemical make-up, which can be configured in a limitless number of ways based on their length and chemical constitution. DNA and RNA consist of a chain of nucleotide building blocks that can be patterned in a vast number of sequences. In the case of DNA, the building blocks are four different nucleotides composed of a five-carbon sugar molecule (deoxyribose), a phosphate group and a nucleobase, which is either adenine (A), thymine (T), guanine (G) or cytosine (C). The nucleotides link together via a sugar-phosphate backbone

to form a single strand of arbitrary sequence such as AGTTCAGGC. Single stranded DNA and RNA has the ability to form a variety of shapes (tertiary structures), due to their ability to form helices and single stranded loops. For a 20 monomer (or 20mer) length, the number of possible configurations is 4^{20} , which is greater than a 1000 billion. These tertiary Aptamer structures bind to their target through non-covalent interactions such as electrostatic interactions, hydrophobic interactions and induced fitting. An evolutionary selection process, called SELEX is used to determine the best nucleotide pattern for specificity to a certain target analyte [22], which can be a wide range of organic biomolecules such as proteins, peptides, small molecules and nucleic acids. They have also been used for the detection of large supramolecular complexes, such as cells and viruses and other entities including nanoparticles, heavy metal ions and tissue.

Whilst aptamers have many advantages they also have some limitations. Their tertiary structures are highly dependent on the solution conditions (e.g. temperature, pH) and presence of any detergents/surfactants. Aptamers are also easily degraded by DNAses or RNAses (enzymes that specifically function to degrade DNA/RNA). This is a particular concern when sensors are used for real-world biological samples (e.g. blood, urine). Other concerns include long discovery time and high cost.

V. NANOGAP ELECTRODES FOR BIOSENSING

The use of nanogap electrodes (namely, a pair of electrodes separated by a very small nanometer-scale gap) for bio-sensing is a common architecture that is widely investigated [23][24]. The central advantage being that high sensitivity can be achieved in the detection of target analytes at very small concentration if the active detecting area of the sensor is of similar size to the target analyte itself. For example, a target analyte passing through two closely spaced (nanogap) electrodes, or immobilized within it, causes a large change in the electrical current passed between the electrodes. Since the dimensions of the nanogap are small, i.e. width and distance between the electrodes, this architecture offers the possibility to detect very small biomolecules with very high sensitivity. Biomolecules capable of detection using this approach include proteins, antibodies, antigens, DNA and viruses. Many types of which have small nanometer sizes and therefore match well the small, active volume of the nanogap electrodes, maximizing the sensitivity.

Another key advantage of the nanogap approach is that the entire electrode architecture, including connecting leads and peripheral circuitry, can have a very small footprint. This allows multiple sensors to be integrated in a small microelectronic chip, that in some cases can be less than the size of a pinhead. Each sensor on the chip can be tailored for the detection of a different target analyte, which for example allows a broad spectrum of diseases to be detected at once, or in some cases, the array of sensors can be configured to detect a characteristic “fingerprint” pattern of similar but different viral strains.

A range of nanogap sensor types are possible, including resistive, capacitive or field-effect and these can be made with a planar or vertical architecture. Electrodes can be made from metals, semiconductors, graphene and carbon nanotubes. Depending on their type, they can also be label-free or involve

labelled species such as those in which the target analyte attaches to nanoparticles, which are detected instead [25].

The vast majority of nanogap biosensors are based on the detection of changes in the electrical resistance of the device [26][27][28], since techniques for the measurement of electrical resistance are widely known, simple to carry out and easy to understand. Capacitive and impedance-based biosensors in contrast are much less studied. However, they are arguably more powerful since they can provide important additional information, through the frequency dependence and phase information.

Whilst nanogaps electrodes have many advantages they can be difficult to fabricate in commercial volumes because of their complex device structure. Also, sensor designers need to be careful to match the sensing area/volume of the device to the concentration of their target analyte since nanosized interrogation sites can lead to very long discovery times. The following sections give a brief overview of nanogap fabrication methods and the two main types of nanogap biosensors, resistive and capacitive sensors.

A. Nanogap Fabrication Methods

Much of the technologies for making nanogap structures has come from the field of molecular electronics, whose central aim is to downscale electronics to the ultimately small building block material, i.e. single atoms and molecules. The basic process of work in the field is to make devices by attaching very small conducting leads to a single molecule for studying its electronic conduction properties and to improve our understanding of the influence of the measurement leads (electronic coupling) on the conduction properties.

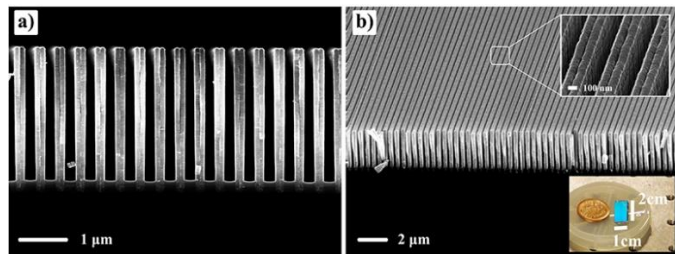


Fig. 11. High aspect ratio TiN nanotrenches made using a combined atomic layer deposition and deep reactive ion etching approach. a) SEM cross-section and b) bird-eye-view. (Reprinted with permission from [29]. Copyright 2017 Optical Society of America)

A major difficulty in the field is to position and attach molecules into devices for studying. Although much work is still progressing in this area, the last two decades have seen a wide variety of methods developed. Aside from techniques involving bulky equipment, such as scanning tunneling microscopy (STM) and conductive atomic force microscopy (AFM), there are a range of methods that permit very small nanogap electrodes to be formed directly on a chip, which is significantly better suited for the development of sensors for applications, in which ease of use and portability is essential. These methods include mechanical controllable break junctions [30], metal electroplating [31], electromigration [32–35] and high aspect ratio nanotrenches made using the shadow evaporation approach [36]. Additionally, there are also a range of methods for making nanogaps using more standard approaches such as electron beam lithography (EBL),

photolithography, nanoimprint lithography [33] and focused ion beam (FIB) milling methods [37][38]. Gap sizes made with these techniques tend to be larger in size than those possible with mechanical controllable break junctions and electromigration techniques. However, if combined with advanced new etching methods and atomic layer deposition, then very small gap sizes with high aspect ratio can be made, such as the nanotrenches shown in Fig. 11.

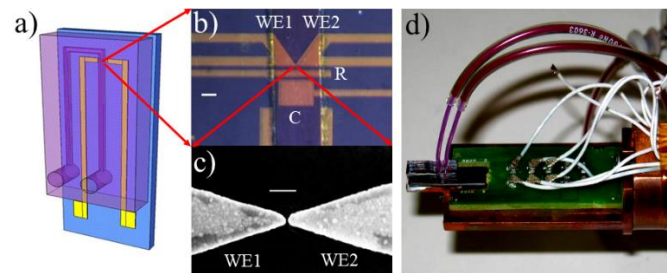


Fig. 12. a) Lab-on-chip metal electroplating within a b) microelectrochemical cell to form c) nanogap electrodes of separation varying from 1-10 nm. The microelectrochemical cell on a silicon substrate contains counter (C), reference (R) and working electrodes (WE1, WE2) and the whole system is integrated with d) microfluidics for simple control of the electroplating fluid and solutions for depositing molecules (Adapted with permission from [31]. Copyright 2011 IOP Publishing Ltd)

Fig. 12 shows the schematic of an approach used to make nanogap electrodes and incorporate molecules into devices using microfluidic control of solutions. The approach consists of a microelectrochemical cell on a silicon wafer, that is made using a combination of photolithography for the conducting leads and electron beam lithography to define a small gap between the two working electrodes. Electrochemical deposition is used to narrow the gap to 1-10 nm for the insertion of molecules of interest. The whole system is integrated with microfluidics for ease of control of the solutions and the systems is mounted on a cryostat finger for rapid cooling and temperature dependent electronic transport studies.

B. Resistive Nanogap Biosensors

The detection of purely resistive changes in electrical resistance is one of the simplest methods used in sensing applications. Electrical resistance is easy to measure and the apparatus can typically be small and low cost. In some cases, a simple handheld instrument such as an ohm meter can suffice.

A change in electrical resistance in these types of nanogap sensors occurs, because there is a change in the overall electrical resistivity of the material within the gap, or, for systems having an inhomogeneous morphology, there is a change in the conduction pathway between the electrodes.

The advantage in having a small separation distance between electrodes lies in the overall change in electrical resistance, which will be maximized when the gap size is tuned to the approximate size of the entity to be detected. Fig. 13 shows one of the earliest sensor types [39]. This device consists of a simple metal-insulator-metal (MIM) design with a separation distance of 5 to 100 nm between the conducting metal electrodes. The distance between the electrodes can be controlled very precisely, ± 1.0 nm, and can be tuned for the length of the analyte to be detected. After deposition of the Au electrodes, two sets of thiol-terminated capture probes with different sequences are immobilized onto the electrodes using wet-chemical self-

assembly methods. The detection process then involves exposure to the target DNA followed by a simple metallization step consisting of the adsorption of silver ions and their reduction by hydroquinone in ammonia to form a conductive silver nanowire. This creates a new primary current pathway, that is substantially different from the background electrical conductivity, when the DNA strand is not present.

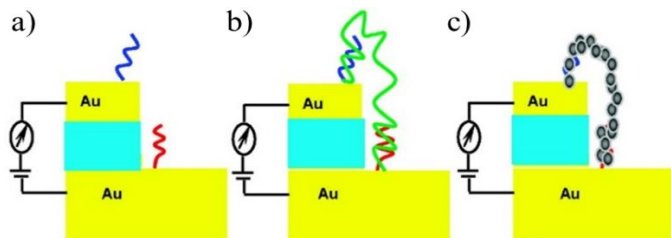


Fig. 13. Schematic of a resistive nanogap sensor showing a) two different capture probes immobilized on the both gold electrodes, b) hybridization of the target DNA (green) followed by c) the formation of an electrically conductive silver pathway for electrical measurement. (Adapted with permission from [39]. Copyright 2009 American Chemical Society)

Another type of approach, but more challenging to fabricate, makes use of the very small diameters of conducting carbon nanotubes as electrodes, as shown in Fig. 14. In this case, a single walled carbon nanotube is oxidatively cut to form a small nanogap. The two ends are then functionalized with 3',5' termini modified DNA molecules via robust amide linkages, which are stable over a wide range of chemistries and conditions. The approach enables two possible configurations, either two different strands are connected, one on each carbon nanotube as shown in Fig. 14a), or a single strand connects across both carbon nanotubes, Fig. 14b). The electrical resistance between the two carbon nanotubes provides a measure of the DNA uptake and hybridization. Significant differences of ~ 300 have been observed [40], depending on the different matched sequences of the two DNA strands, which enables the approach to be used to detect changes in the DNA sequence between the probe and target DNA.

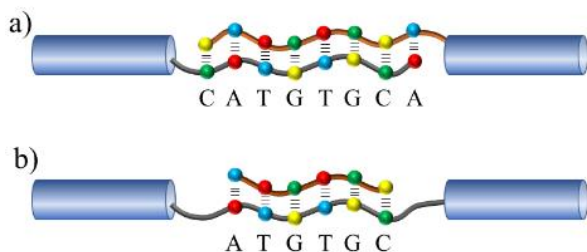


Fig. 14. A nanogap sensor approach based on a single walled carbon nanotube which is oxidatively cut to make point contacts. The device works in two possible configurations, a) two different single DNA strands are connected to opposite carbon nanotubes or b) a single strand is used to make an electrical connection across both carbon nanotubes. Measurements of the electrical resistance are used to assess the hybridization quality of the two DNA strands, which is a measure of differences between the target and probe DNA sequences.

Nanogap electrodes have also been integrated within a field-effect transistor (FET)-type to make a new type biosensor [41], that has some similarities to the ion-sensitive FET (ISFET) that was first invented in 1970 and since used for measuring ion concentrations in solutions [42]. In this new

nanogap-based design, a unique suspended architecture is utilized involving a 500 nm thick conductive poly-Si gate electrode that is suspended above a 20 nm nanogap, as shown in Fig. 15. Underneath the nanogap an insulating SiO_2 layer functionalized with silica-binding proteins (SBP) is used as a surface for capturing the target analyte. The SBP binds strongly to the SiO_2 surface at one end and fuses to an antibody probe at the other end. The antibody facilitates the immobilization of the target antigen biomolecule. Electronic sensing is achieved because the binding of the antigen to the SiO_2 gate oxide increases the dielectric constant of the nanogap region, causing the gate capacitance to increase. The gate capacitance directly effects the conduction of the drain-source channel, which is controlled by the gate voltage. By fixing the drain current to be constant at 10 nA and monitoring changes in the gate voltage that is required to keep this current constant, the capture of specific biomolecules in the nanogap can be monitored. The main advantage of the nanogap FET is its bridge-like suspended gate, which allows biomolecules to move freely in and out of the nanogap channel beneath it. The nanogap can also be tuned to the target biomolecule size.

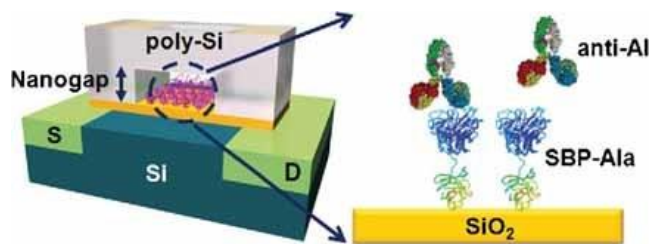


Fig. 15. A FET device consisting of a suspended poly-Si gate above a nanogap region in which biomolecules can pass freely through. Immobilization of targets species on the bottom SiO_2 functionalized layers changes the dielectric constant of the nanogap region which effects the conduction properties in the source-drain channel. (Reproduced from ref. [41] by permission of © 2009 WILEY-VCH Verlag GmbH & Co. KGaA, Weinheim)

The use of nanogap electrodes can also serve the dual purpose of both electrical measurements and the positioning of biomolecules into the desired regions of the device. Dielectrophoresis (DEP) is a phenomenon that causes a force to be exerted on a dielectric particle in the presence of a non-uniform electric field. It can have great selectivity and has been used for the separation of cells, proteins and strains of bacteria and virus. DEP also works with nanoparticles and has been used to position them into the spaces between nanogap electrodes.

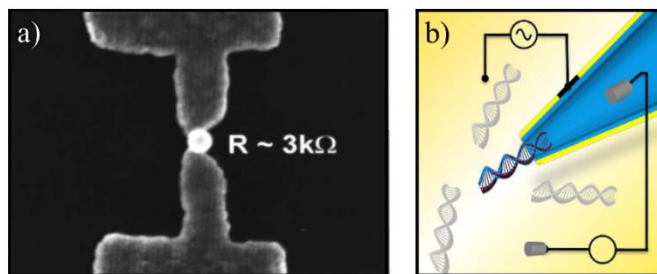


Fig. 16. Dielectrophoresis applied a) to the capturing and measurement of a single 80 nm diameter Au nanoparticle within a nanogap electrode (Reprinted from [25], with the permission of AIP Publishing) and b) its recent use in nanopores where it can be used to manipulate and measure single DNA molecules (Reprinted with permission from [43])

Early work in the use of DEP in nanogap electronics was in the field of molecular electronics [25]. Fig. 16a) shows how an alternating AC potential of 0.5–2.5 V (peak-to-peak) with frequency ranging from 1 to 10 MHz was applied across nanogap electrodes to impart a dielectrophoretic force on an Au nanoparticle to position it within a nanogap. The effect was found to work on nanoparticles with diameters ranging from 40 to 100 nm. After trapping, electrical measurement between the electrodes was then used to measure the resistance of the nanoparticle, which had a functionalized surface with the molecules of interest for the study. Although this work was initially focussed on molecular electronics studies, DEP has since been applied to the positioning and electrical detection of DNA and proteins [44] in nanogap devices. In recent years the use of DEP for the positioning of biomolecules has grown enormously across a wide range of applications. Particular interesting is the development of new DEP technologies such as nanopipettes [45] and nanopores [43] (see Fig. 16.b) that can be used for both, positioning and detecting single proteins and DNA molecules. It is hoped that one day these technologies may lead to the ability to sequentially read and discriminate between nucleotide types on a DNA chain with high throughput [46][47].

C. Capacitive Nanogap Biosensors

Capacitive sensors based on the detection of recognized entities in close proximity of the electrodes, called capacitive affinity sensors, first started appearing in the mid-1980s [48]. They function by detecting changes in the dielectric properties of the region between two electrodes when an analyte binds, as shown in Fig. 17. A bio-recognition element (e.g. antibody) is used to immobilize the specific analyte of interest (e.g. antigen), whose presence causes a change in the dielectric properties of the material between the two electrodes. This is measured by detecting the change in the capacitance between the two plates.

The governing equation for a parallel plate capacitor, that relates the dielectric properties of the media between the plates to the capacitance is $C = \epsilon_r \epsilon_0 A / d$, where ϵ_r is the relative dielectric constant of the material within the gap, ϵ_0 is the permittivity of free space, A is the electrode area and d is their separation. The change in capacitance will be evident because there is a change in the material between the two electrodes, which will need to have a different ϵ_r , compared to the original solution. The overall change in capacitance will be maximized when the entity (i.e. molecule, protein, antigen etc...) has a very different dielectric polarizability to the material displaced (i.e. electrolyte, buffer solution, water etc.) and when the volume of material exchanged is a maximum.

Although these devices have had many successful applications, they have several drawbacks. One of these is that they suffer from large electrode polarization effects because of their large, macroscopic sized electrodes [49]. Electrode polarization arises because of movement of free ions to the electrode-solution interface, where they form an electrical double layer (EDL). The EDL limits the detection capabilities of the sensor since the capacitance of this layer dominates the signal at low frequency, masking relaxation effects in the

bulk [50] and leading to incorrect measurement of the capacitance (or relative permittivity), as shown in Fig. 18.

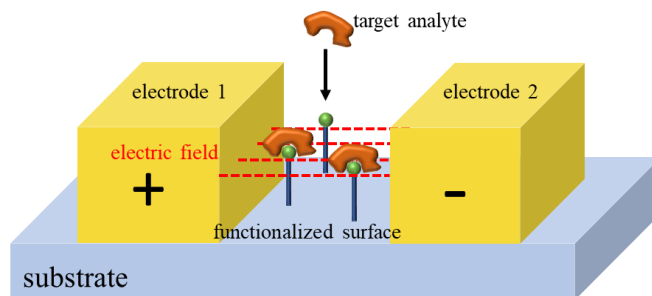


Fig. 17. Capacitive affinity sensor based on two metal electrodes separated by a gap. A bio-recognition element causes the immobilization of the analyte, which changes the dielectric properties between the two electrodes.

Previously, the determination of the true dielectric properties of a material or biological entity of interest in a liquid environment, has relied on methods of either correcting the measured data, or physically compensating the electrode double layer. Analytical correction [51][52] typically involves the fitting of known empirical functions, or, for more complex studies, the electrode polarization can be modelled using long-range many-body theory. In the case of physical mechanisms, the EDL can be compensated through the use of reference electrodes, or the insertion of thin electrically insulating blocking electrodes [53][54]. However, both analytical and physical based approaches have a number of flaws and no simple correction technique exists to cover all scenarios. This is because the electrode polarization effect is very complex and highly dependent on the chemistry, involving both the electrolyte and electrode materials, as well as the nature of the electrodes surface and its topography. The distribution of ions is also important and involves both short and long-range interactions of ions at the electrode/solution interface.

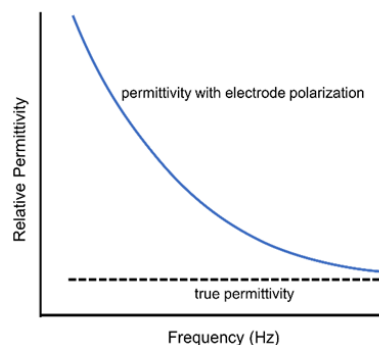


Fig. 18. Eliminating the effects of electrode polarization reveals the true dielectric properties of the material contained within the nanogap electrodes. (Reproduced from Ref. [55] with permission from the PCCP Owner Societies.)

In recent years an alternative approach, based on nanogap electrodes has evolved, that eliminates the need for analytical and physical compensation. The method allows the true capacitance to be determined directly through electrical measurements without any compensation.

The first efforts towards using nanogap electrodes for eliminating the EDL parasitic effect appeared in 2005 with the work setting out the main theoretical concept as well as first experimental results [56]. The main idea of the approach was that decreasing the gap size between two opposite electrodes

containing an electrolyte would cause the two EDLs to interact with each other due to the space confinement. By treating the ions in the EDL in terms of the Gouy–Chapman model and solving the Poisson–Boltzmann equation for the electrical potential, modelling studies revealed that the overlapping EDL interaction of two closely spaced electrodes minimizes the contribution of the EDL to the measured capacitance. For nanogap electrodes having an electrode separation, L , which is less than the electrical double layer thickness, such that $L \sim 0.1 \kappa^{-1}$ (where κ is the Debye–Hückel parameter and κ^{-1} is the Debye length), the electrical potential across the nanogap varies as shown in the non-dimensionalized plot in Fig. 19, where S_n represents the size of the nanogap relative to the Debye length, and Φ is the potential at position x within the gap and where x is normalized by the nanogap gap length. It is evident that, when $S_n = 0.1$, the potential is constant across the gap, which means the measured capacitance is no longer dominated by the interfacial charge separation. A schematic of the effect of reducing the nanogap electrode separation to cause the two electrical double layers to overlap is shown in Fig. 20.

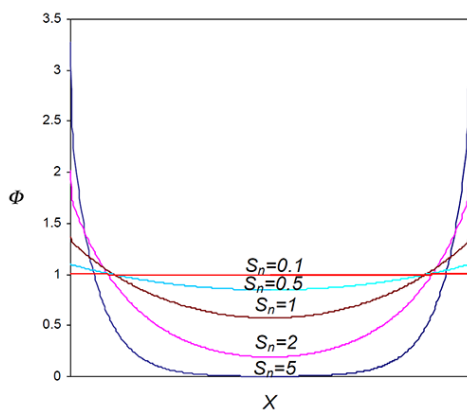


Fig. 19. Electrical potential (Φ) as a function of position (x) across nanogaps with various sizes relative to the Debye length (S_n). The potential in the middle of the gap decreases as the gap size increases while the potential on the electrode surfaces increases. A uniform potential across the nanogap is obtained when the gap size is smaller than the electrical double layer thickness, as shown when $S_n = 0.1$ (Reprinted from [56] © 2004, with permission from Elsevier B.V.)

This first study on overlapping the EDLs to overcome electrode polarization effects was also aimed at developing a new biosensor type. Nanogap capacitor devices containing various ionic strength electrolytes were first studied for their low frequency response. This was followed by investigations on the use of the device as a biosensor for the detection of single stranded DNA oligonucleotides with 20-mer length. The work was able to show changes in capacitance at concentrations of ssDNA in aqueous solutions as low as 100 nM. Altogether, this pioneering work was significant in demonstrating not only the advantages of using nanogap electrodes to reduce electrode polarization effects, but also how critically important this is when using capacitance as an indicator of the presence of biomolecules for biosensing applications.

A significant improvement in the approach came in 2010, when the nanogap concept was combined with surface functionalization to directly address the issue of immobilization of target analytes within the desired region of the device. In this work [57], the authors moved away from the use of highly doped silicon as the electrode material, as used in the earlier

study, to gold electrodes, which allowed the use of thiol bonded DNA aptamers to be directly integrated onto the electrodes of the device. This combination of the nanogap spaced electrodes with aptamer functionalization proved to be a powerful method, allowing the label-free detection of protein molecules with high sensitivity and high specificity. The work utilized a new vertical nanogap structure that allowed both electrodes to be metal for aptamer functionalization and successfully demonstrated the use of the nanogap capacitor for the detection of human alpha thrombin with concentrations as low as 1 μ M.

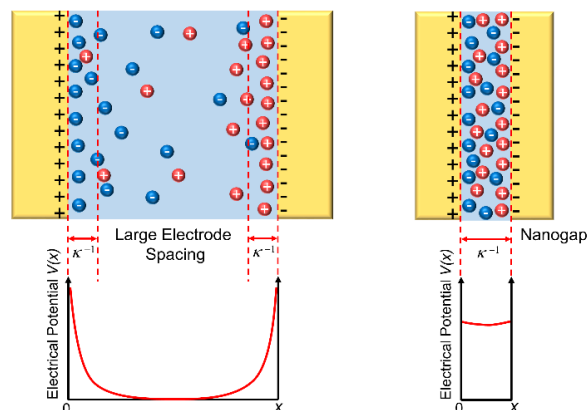


Fig. 20. Overlapping electrical double layers leads to a constant electrical potential across a nanogap device, eliminating electrode polarization effects. (Reproduced from Ref. [55] with permission from the PCCP Owner Societies.)

Recently, a simpler approach has been developed to fabricate the nanogap capacitor biosensors. The method supports the use of low cost glass substrates and involves only a simple two-step photolithography process and a single HF etching step [55]. It does not require the deposition of a SiN_3 layer and also eliminates the need of a complicated electrode planarization process, that involves both, chemical-mechanical polishing and the deposition of large amounts of gold, which is costly for large scale production (two 1 μ m thick gold evaporations in contrast to two 50 nm gold evaporations). The process reverts back to the original architecture, a horizontal nanogap with electrodes vertically stacked, but has the advantage of metal electrodes, which allows surface functionalization using thiol modified aptamers. The device architecture, shown in Fig. 21a), involves first the deposition of gold bottom electrodes using photolithography, followed by the deposition of a SiO_2 support layer. After deposition of the top gold electrode, a chemical etching step is used to remove sections of the underlying SiO_2 . The final device, which is smaller than the thickness of a human hair (<100 μ m), combines 100 nanogap capacitors in parallel, Fig. 21b), to give a sufficiently high device capacitance for good signal to noise ratio measurements and the use of simple and low-cost electronic measurement instrumentation.

The device was shown to be effective in operating as a biosensor and was used to successfully detect human alpha thrombin with concentrations as low as 1 μ M, as shown in Fig. 21c). Although, other sensor types routinely detect fM/pM concentrations, the sensor in this report had not been optimized to achieve its ultimate limit of sensitivity, which is expected to be in the vicinity of the attomolar range (see [55] for discussion). Instead, the focus of the research was to validate the advantage of overlapping the EDLs to permit low frequency measurements and true quantification of the dielectric

permittivity of the material within the gap. Additionally, it provided simpler approaches for device fabrication and gave new understanding to important differences seen in previous studies, when the nanogap contained only air and water.

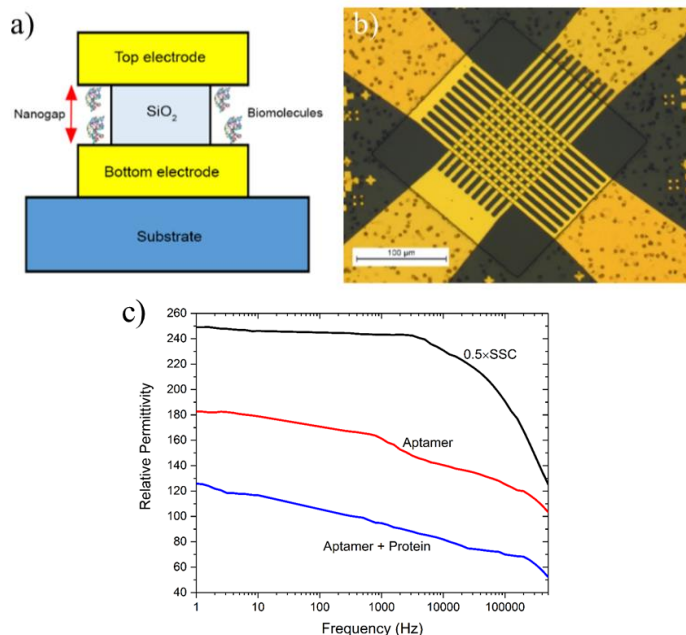


Fig. 21. A label-free aptamer-based nanogap capacitive biosensor having greatly diminished electrode polarization effects and targeted for the detection of human alpha thrombin. a) Schematic showing the vertical structured nanogap with a central SiO₂ support structure and 40 nm separated nanogap between gold electrodes. b) Top-down view of the device that is 100 μm wide and contains 100 capacitors measured in parallel. c) Relative permittivity vs log (frequency) for a bare nanogap device in the presence of a 0.5x SSC buffer (black curve), after surface functionalization with the single strand DNA aptamer (red curve), measured again in 0.5x SSC buffer, and after binding with human α-thrombin protein (concentration 1 μM in 0.5xSSC buffer solution). (Reproduced from Ref. [55] with permission from the PCCP Owner Societies.)

Overall, the use of nanogap spaced electrodes to remove electrode polarization effects in capacitive measurements is still an emerging area and much work remains to be done in the field. For applications, further research should be aimed at simplifying the fabrication process for high throughput commercial manufacture, whilst also improving device yield and robustness. Research should also examine how devices could be reused multiple times. In theory, target molecules will dissociate from the aptamer at higher temperature or a change in pH, allowing potential reuse of the device. A change in temperature or pH might however negatively affect device functionality and sensitivity, but as of yet, few studies have been done. Fundamental studies also need to be done to further the understand the effect of confining liquids in nanoscale cavities. Especially when there are strong surface interactions and electric fields present, that may be of sufficient strength to cause changes in the liquid structure (crystallinity) and therefore measured dielectric properties.

VI. CONCLUSION

Recent advances in nanofabrication offer many benefits for the development of new sensing technologies. This tutorial has focused on electrochemical impedance spectroscopy and nanoscale sensing technologies that use electrodes separated by

a very small nanometer-scale gap. The reduction of the gap size to nanoscale lengths provides enormous advantages for the detection of surface bound species. The basic tenet being that the size of the measurement device (electrodes) is similar to that of the species being detected, which will therefore elicit a large detection response. When combined with surface functionalization of the electrodes, the detection response can be further refined to be not only extremely sensitive but also highly specific to the biomolecule targeted for detection.

Two main nanogap electrode types have been reviewed, resistive and capacitive sensors. The detection of purely resistive changes is the simplest method and enables the use of small, low cost, handheld equipment. Newer capacitive sensing, although more challenging, holds great promise for the future. The reduction of the electrode gap spacing to lengths smaller than the Debye length causes the electrode double layers to overlap, which minimizes electrode polarization effects and its associated parasitic capacitance, which is a common problem of macroscopic sized capacitive biosensors. This enables true quantification of the permittivity of the material between the nanogap and the use of low frequency electrical measurements. The latter may prove to be particularly important, since it could be used to detect large-scale changes in molecular structures, such as binding events and conformation changes in target species such as DNA.

REFERENCES

- Cardoso, A.R., Moreira, F.T.C., Fernandes, R., Sales, M.G.F.: Novel and simple electrochemical biosensor monitoring attomolar levels of miRNA-155 in breast cancer. *Biosens. Bioelectron.* 80, 621–630 (2016)
- Campos, R., Borme, J., Guerreiro, J.R., Machado, G., Cerqueira, M.F., Petrovykh, D.Y., Alpuim, P.: Attomolar label-free detection of dna hybridization with electrolyte-gated graphene field-effect transistors. *ACS Sensors*. 4, 286–293 (2019)
- Tzouavadaki, I., Jolly, P., Lu, X., Ingebrandt, S., De Micheli, G., Estrela, P., Carrara, S.: Label-free ultrasensitive memristive aptasensor. *Nano Lett.* 16, 4472–4476 (2016)
- Hwang, M.T., Heiranian, M., Kim, Y., You, S., Leem, J., Taqieddin, A., Faramarzi, V., Jing, Y., Park, I., van der Zande, A.M., Nam, S., Aluru, N.R., Bashir, R.: Ultrasensitive detection of nucleic acids using deformed graphene channel field effect biosensors. *Nat. Commun.* 11, (2020)
- da Silva, E.T.S.G., Souto, D.E.P., Barragan, J.T.C., de F. Giarola, J., de Moraes, A.C.M., Kubota, L.T.: Electrochemical Biosensors in Point-of-Care Devices: Recent Advances and Future Trends. *ChemElectroChem*. 4, 778–794 (2017)
- Coskun, A.F., Topkaya, S.N., Yetisen, A.K., Cetin, A.E.: Portable Multiplex Optical Assays. *Adv. Opt. Mater.* 7, 1–25 (2019)
- Volta, A.: On the electricity excited by the mere contact of conducting substances of different kinds. In a letter from Mr. Alexander Volta, F.R.S., professor of natural philosophy in the University of Pavia, to the Rt. Hon. Sir Joseph Banks, Ban, K.B.P.R.S. . *Phil. Trans. R. Soc. L.* 90, 744–746 (1800)
- Varley, C.E.F.: VII. Polarization of metallic surfaces in aqueous solutions. On a new method of obtaining electricity from mechanical force, and certain relations between electrostatic induction and the decomposition of water. *Philos. Trans. R. Soc. London.* 161, 129–136 (1871)
- Helmholtz, H.: Studien uber elektrische Grenzschichten. *Ann. Phys. Chem.* 7, 337–382 (1879)
- Warburg, E.: Ueber das Verhalten sogenannter unpolarisierbarer Elektroden gegen Wechselstrom. *Ann. Phys. Chem.* 67, 493–499 (1899)
- Fricke, H.: The theory of electrolytic polarization. *Phil. Mag.* 14, 310–318 (1932)
- Randles, J.E.B.: Kinetics of rapid electrode reactions. *Discuss. Faraday Soc.* 1, 11 (1947)
- Helmholtz, H.: Ueber einige Gesetze der Vertheilung elektrischer Ströme in körperlichen Leitern mit Anwendung auf die thierischelektrischen Versuche. *Pogg Ann.* 89, 211–33, 352–77, Repr. in *WA 1* pp.475-519

- (1853)
14. Gouy, G.: Sur la constitution de la charge électrique à la surface d'un électrolyte. *J. Phys. Radium*. 9, 457–468 (1910)
 15. Chapman, D.L.: A contribution to the theory of electrocapillarity. *Philos. Mag.* 25, 475–481 (1913)
 16. Stern, O.: Zur Theorie Der Elektrolytischen Doppelschicht. *Zeitschrift für Elektrochemie*. 30, 508–516 (1924)
 17. Grahame, D.C.: Capacity of the Electrical Double Layer between Mercury and Aqueous Sodium Fluoride. II. Effect of Temperature and Concentration. *J. Am. Chem. Soc.* 79, 2093–2098 (1957)
 18. Stern, E., Klemic, J.F., Routenberg, D.A., Wyrembak, P.N., Turner-Evans, D.B., Hamilton, A.D., LaVan, D.A., Fahmy, T.M., Reed, M.A.: Label-free immunodetection with CMOS-compatible semiconducting nanowires. *Nature*. 445, 519–522 (2007)
 19. Jolly, P., Tamboli, V., Harniman, R.L., Estrela, P., Allender, C.J., Bowen, J.L.: Aptamer-MIP hybrid receptor for highly sensitive electrochemical detection of prostate specific antigen. *Biosens. Bioelectron.* 75, 188–195 (2016)
 20. Poghossian, A., Schöning, M.J.: Label-Free Sensing of Biomolecules with Field-Effect Devices for Clinical Applications. *Electroanalysis*. 26, 1197–1213 (2014)
 21. Balamurugan, S., Obubuafo, A., Soper, S.A., Spivak, D.A.: Surface immobilization methods for aptamer diagnostic applications. *Anal. Bioanal. Chem.* 390, 1009–1021 (2008)
 22. Zhuo, Z., Yu, Y., Wang, M., Li, J., Zhang, Z., Liu, J., Wu, X., Lu, A., Zhang, G., Zhang, B.: Recent advances in SELEX technology and aptamer applications in biomedicine. *Int. J. Mol. Sci.* 18, 1–19 (2017)
 23. Li, T., Hu, W., Zhu, D.: Nanogap Electrodes. *Adv. Mater.* 22, 286–300 (2010)
 24. Chen, X., Guo, Z., Yang, G., Li, J., Li, M., Liu, J., Huang, X.: Electrical nanogap devices for biosensing. *Mater. Today*. 13, 28–41 (2010)
 25. Amlani, I., Rawlett, A.M., Nagahara, L.A., Tsui, R.K.: An approach to transport measurements of electronic molecules. *Appl. Phys. Lett.* 80, 2761–2763 (2002)
 26. Kim, S.K., Cho, H., Park, H., Kwon, D., Lee, J.M., Chung, B.H.: Nanogap biosensors for electrical and label-free detection of biomolecular interactions. *Nanotechnology*. 20, 455502 (2009)
 27. Zhang, H., Xu, W., Liu, X., Stellacci, F., Thong, J.T.L.: Capturing a DNA duplex under near-physiological conditions. *Appl. Phys. Lett.* 97, 163702 (2010)
 28. Tsutsui, M., Taniguchi, M., Yokota, K., Kawai, T.: Identifying single nucleotides by tunnelling current. *Nat. Nanotechnol.* 5, 286–290 (2010)
 29. Shkondin, E., Repán, T., Takayama, O., Lavrinenko, A. V.: High aspect ratio titanium nitride trench structures as plasmonic biosensor. *Opt. Mater. Express*. 7, 4171 (2017)
 30. Reed, M.A., Zhou, C., Muller, C.J., Burgin, T.P., Tour, J.M.: Conductance of a Molecular Junction. *Science*. 278, 252–254 (1997)
 31. Lunc-Popa, P., Dalmas, G., Faramarzi, V., Dayen, J.F., Majjad, H., Kemp, N.T., Doudin, B.: Heteronanojunctions with atomic size control using a lab-on-chip electrochemical approach with integrated microfluidics. *Nanotechnology*. 22, (2011)
 32. Park, H., Lim, A.K.L., Alivisatos, A.P., Park, J., McEuen, P.L.: Fabrication of metallic electrodes with nanometer separation by electromigration. *Appl. Phys. Lett.* 75, 301–303 (1999)
 33. Gee, A., Jaafar, A.H., Kemp, N.T.: Nanoscale Junctions for Single Molecule Electronics Fabricated using Bilayer Nanoimprint Lithography combined with Feedback Controlled Electromigration. *Nanotechnology*. 31, 155203 (2020)
 34. Gee, A., Jaafar, A.H., Brachňáková, B., Massey, J., Marrows, C.H., Šalitroš, I., Kemp, N.T.: Multilevel Resistance Switching and Enhanced Spin Transition Temperature in Single- and Double-Molecule Spin Crossover Nanogap Devices. *J. Phys. Chem. C*. 124, 13393–13399 (2020)
 35. Beaufrand, J.-B., Dayen, J.-F., Kemp, N.T., Sokolov, A., Doudin, B.: Magnetoresistance signature of resonant states in electromigrated Ni nanocontacts. *Appl. Phys. Lett.* 98, 142504 (2011)
 36. Dayen, J.-F., Faramarzi, V., Pauly, M., Kemp, N.T., Barbero, M., Pichon, B.P., Majjad, H., Begin-Colin, S., Doudin, B.: Nanotrench for nano and microparticle electrical interconnects. *Nanotechnology*. 21, 335303 (2010)
 37. Kemp, N.T., McGrouther, D., Cochrane, J.W., Newbury, R.: Bridging the gap: Polymer nanowire devices. *Adv. Mater.* 19, 2634–2638 (2007)
 38. Kemp, N.T., Newbury, R., Cochrane, J.W., Dujardin, E.: Electronic transport in conducting polymer nanowire array devices. *Nanotechnology*. 22, 105202 (2011)
 39. Roy, S., Chen, X., Li, M.H., Peng, Y., Anariba, F., Gao, Z.: Mass-produced nanogap sensor arrays for ultrasensitive detection of DNA. *J. Am. Chem. Soc.* 131, 12211–12217 (2009)
 40. Guo, X., Gorodetsky, A.A., Hone, J., Barton, J.K., Nuckolls, C.: Conductivity of a single DNA duplex bridging a carbon nanotube gap. *Nat. Nanotechnol.* 3, 163–167 (2008)
 41. Gu, B., Park, T.J., Ahn, J.H., Huang, X.J., Lee, S.Y., Choi, Y.K.: Nanogap field-effect transistor biosensors for electrical detection of avian influenza. *Small*. 5, 2407–2412 (2009)
 42. Bergveld, P.: Development of an Ion-Sensitive Solid-State Device for Neurophysiological Measurements. *IEEE Trans. Biomed. Eng.* BME-17, 70–71 (1970)
 43. Freedman, K.J., Otto, L.M., Ivanov, A.P., Barik, A., Oh, S.H., Edel, J.B.: Nanopore sensing at ultra-low concentrations using single-molecule dielectrophoretic trapping. *Nat. Commun.* 7, 1–9 (2016)
 44. Zheng, L., Brody, J.P., Burke, P.J.: Electronic manipulation of DNA, proteins, and nanoparticles for potential circuit assembly. *Biosens. Bioelectron.* 20, 606–619 (2004)
 45. Jia, R., Mirkin, M. V.: The double life of conductive nanopipette: A nanopore and an electrochemical nanosensor. *Chem. Sci.* 11, 9056–9066 (2020)
 46. Tian, K., Decker, K., Aksimentiev, A., Gu, L.Q.: Interference-Free Detection of Genetic Biomarkers Using Synthetic Dipole-Facilitated Nanopore Dielectrophoresis. *ACS Nano*. 11, 1204–1213 (2017)
 47. Bowden, R., Davies, R.W., Heger, A., Pagnamenta, A.T., de Cesare, M., Oikkonen, L.E., Parkes, D., Freeman, C., Dhalla, F., Patel, S.Y., Popitsch, N., Ip, C.L.C., Roberts, H.E., Salatino, S., Lockstone, H., Lunter, G., Taylor, J.C., Buck, D., Simpson, M.A., Donnelly, P.: Sequencing of human genomes with nanopore technology. *Nat. Commun.* 10, 1–9 (2019)
 48. Newman, A.L., Hunter, K.W., Stanbro, W.D.: *Chemical Sensors: 2nd International Meeting Proceedings*. (1986)
 49. Daniels, J.S., Pourmand, N.: Label-Free Impedance Biosensors: Opportunities and Challenges. *Electroanalysis*. 19, 1239–1257 (2007)
 50. Ishai, P. Ben, Talary, M.S., Caduff, A., Levy, E., Feldman, Y.: Electrode polarization in dielectric measurements: a review. *Meas. Sci. Technol.* 24, 102001 (2013)
 51. Schwan, H.P.: Linear and nonlinear electrode polarization and biological materials. *Ann. Biomed. Eng.* 20, 269–288 (1992)
 52. Kornyshev, A.A.: Double-layer in ionic liquids: Paradigm change? *J. Phys. Chem. B*. 111, 5545–5557 (2007)
 53. Pizzitutti, F., Bruni, F.: Electrode and interfacial polarization in broadband dielectric spectroscopy measurements. *Rev. Sci. Instrum.* 72, 2502–2504 (2001)
 54. Jansson, H., Bergman, R., Swenson, J.: Hidden slow dynamics in water. *Phys. Rev. Lett.* 104, 017802 (2010)
 55. Namhil, Z.G., Kemp, C., Verrelli, E., Iles, A., Pamme, N., Adawi, A.M., Kemp, N.T.: A Label-Free Aptamer-Based Nanogap Capacitive Biosensor with Significantly Diminished Electrode Polarization Effects. *PCCP*. 21, 681–691 (2019)
 56. Yi, M., Jeong, K.H., Lee, L.P.: Theoretical and experimental study towards a nanogap dielectric biosensor. *Biosens. Bioelectron.* 20, 1320–1326 (2005)
 57. Mannoor, M.S., James, T., Ivanov, D. V., Beadling, L., Braunlin, W.: Nanogap dielectric spectroscopy for aptamer-based protein detection. *Biophys. J.* 98, 724–732 (2010)



Neil Kemp is a Reader in Physics at the University of Hull, U.K. He received his PhD from Victoria University of Wellington (NZ) in 2000, before carrying out postdoctoral work at the University of New South Wales (Australia) and IPCMS, Strasbourg (France). In 2009, he established a Nanophysics research group at the University of Hull with a focus on nanotechnology for real-world electronic applications. His current area of focus is optical memristors for neuromorphic computing, and nanoscale engineering for single molecule spintronics and bio-sensing. During 2020-21 he was a Senior Visiting Research Fellow at the Technische Universität Dresden (Germany) (for more details see our group webpage - kempnanogroup.com).